Doctoral Dissertation (Censored)
博士論文（要約）

Roles of Rossby wave and gravity wave generation in the middle atmosphere in the interhemispheric coupling
（南北半球間結合における中層大気での
ロスビー波および重力波発生の役割）

A Dissertation Submitted for the Degree of Doctor of Philosophy
February 2020
令和 2 年 2 月　博士（理学）申請

Department of Earth and Planetary Science,
Graduate School of Science, The University of Tokyo
東京大学　大学院理学系研究科　地球惑星科学専攻

Ryosuke Yasui
安　井　良　輔

Abstract

Stratospheric Sudden Warmings (SSWs) often occur at the polar region in the winter northern hemisphere (NH). This is a phenomenon in which a Lagrangian mean meridional circulation in the NH stratosphere is driven by forcing of stationary Rossby waves (RWs) originating from the troposphere, resulting in adiabatic heating (cooling) in the Arctic (equatorial) stratosphere. It has been reported using satellite observations that warming at high latitudes in the summer mesosphere and lower thermosphere (MLT) of the southern hemisphere (SH) appears during an Arctic SSW. This phenomenon has also been confirmed using numerical model simulations. Based on these results, a scenario of interhemispheric coupling of temperature anomaly through the regions from the NH stratosphere and mesosphere to the SH MLT region has been proposed. This scenario describes that the interhemispheric coupling occurs due to the modulation of mesospheric meridional circulation driven by forcing of gravity waves (GWs) originating from the troposphere. On the other hand, when the warm anomaly is formed at NH high latitudes in the stratosphere, a cold anomaly is formed over the region across the equator to SH low latitudes in the stratosphere. Moreover, the quasi 2-day waves (QTDWs), which are identified as Rossby-gravity normal mode with $(s,\ n-s) = (3, 0)$ and give strong wave forcing in the SH mesosphere, develop during an SSW, resulting in warming at SH mid-latitudes in the upper mesosphere. These features show that the previous scenario of the interhemispheric coupling may not be complete. Recently, it is also shown that RWs and GWs are respectively generated from the barotropic (BT) and/or baroclinic (BC) instability in the winter mesosphere and from the shear instability in the summer mesosphere. These RWs and GWs generated in-situ in the mesosphere may largely influence the momentum budget in the MLT region. This study revisits the

interhemispheric coupling following the NH SSWs from a viewpoint of wave forcing not only by GWs and RWs originating from the troposphere but also by GWs, RWs, and Rossby-gravity waves (RGWs) generated in-situ in the middle atmosphere. This study also elucidates causes of the warm anomaly in the SH MLT region that occurs in the interhemispheric coupling.

In this study, data for the neutral atmosphere from simulations by a whole atmosphere model called Ground–to–topside model of Atmosphere and Ionosphere for Aeronomy (GAIA) are analyzed. The model resolution is T42L150. Orographic and non-orographic GW parameterizations are included. The model is nudged by the Japanese 25-year Reanalysis (JRA-25)/Japan Meteorological Agency Climate Data Assimilation System (JCDAS) data below about a height of 30 km. The analyzed time period is 19 boreal winter seasons in the time period of December 1996 to March 2015. The analyzed height region is from the surface to 120 km. To validate the reality of the model fields in the stratosphere and lower mesosphere, Aura Microwave Limb Sounder (MLS) observation and Modern-Era Retrospective analysis for Research and Applications Version 2 (MERRA-2) data are also analyzed.

The interhemispheric coupling events are extracted as cold equatorial stratosphere events: first, a temperature anomaly from the climatology is calculated. A 90-day running mean is removed from the temperature anomaly (hereafter referred to as "anomaly") to exclude the effects of 11-year solar activity cycle. Second, the time period of the cold equatorial stratosphere events is defined as that during which the temperature anomalies at (0 °N, 5 hPa) and (20 °S, 5 hPa) are lower than twice of the standard deviation ($\sigma_{0\,^\circ\mathrm{N}}$ and $\sigma_{20\,^\circ\mathrm{S}}$), and the day with the coldest anomaly is defined as the central day (Day = 0). A composite analysis is performed for the anomaly of the

temperature, wind, potential vorticity, wave activity flux, and wave forcing. The disturbances are divided into three as follows: first, migrating tides with zonal wavenumber 1–3 are extracted from the original data as a tidal component. Second, using Fourier analysis, the remaining component is divided into RWs/RGWs with wave periods longer than 24 hours and (resolved) GWs with wave periods shorter than or equal to 24 hours. The contribution of each wave forcing to the momentum budget is examined.

First, the temperature, wind, wave activity, and wave forcing are analyzed from a viewpoint of zonal mean fields. The cold anomaly in the equatorial stratosphere extends latitudinally to about 40 °S. This is caused by a strong wave forcing in the NH stratosphere. When the cold equatorial stratosphere occurs, a warm anomaly first appears at SH high latitudes in the lower thermosphere (Day = +4). Subsequently, the warm anomaly region moves down to the SH upper mesosphere (Day = +9). Compared with the wave forcing anomaly due to GWs and RWs/RGWs, these warm anomalies in the SH MLT region are caused by resolved GWs for the lower thermosphere and by RWs/RGWs, especially QTDWs, for the upper mesosphere. Therefore, the interhemispheric coupling seems to occur through a different mechanism from that proposed by the previous studies. Furthermore, it is also revealed that QTDWs and resolved GWs that cause the warm anomalies in the SH MLT region are radiated respectively from BT/BC instability and from shear instability in the mesosphere. These instabilities are formed by parameterized GW forcing, namely, GWs originating from the SH troposphere. It is suggested that the parameterized GW forcing is modulated by the westward wind anomaly in the SH stratosphere.

Previous observations and numerical simulations showed that there is a wide range of time lag of ~5–10 days between the appearance of the temperature and wave

forcing anomalies in the NH stratosphere and that of the temperature anomaly in the SH MLT region and that the time lag depends on the season. In this study, there is a long-time lag of ~5 days between the date of the warm anomaly maximum in the SH lower thermosphere and that in the SH upper mesosphere on average. This result is consistent with the time lag shown in the previous observational studies. This may be because QTDWs need a longer time (several days) to develop in the mesosphere and propagate to the upper mesosphere than resolved GWs (approximately 1 day). As shown by the previous studies, the seasonality of the growth rate of the QTDWs is large, and the QTDWs hardly develop in the first half of December and the second half of February. Thus, it is considered that the wide range of the time lag and its seasonality of the time lag reported in the previous studies are due to the fact that the two types of waves (i.e., GWs and QTDWs) play important roles in the interhemispheric coupling.

Next, causes of the cold anomaly in the equatorial stratosphere are examined by comparing strong cold events with weak cold events. This cold anomaly is important to form the westward wind anomaly at SH low and mid-latitudes in the stratosphere and mesosphere. A negative wave forcing anomaly in the NH upper stratosphere and lower mesosphere is extended to NH low latitudes during the strong cold equatorial stratosphere events. The negative wave forcing anomaly strengthens the middle atmosphere Hadley circulation. The strengthened middle atmosphere Hadley circulation causes upward flow anomaly in the equatorial stratosphere. The negative wave forcing anomaly at NH low latitudes is caused by the breaking of the stationary RWs with zonal wavenumber s = 1 originating from the troposphere and by the generation of secondary RWs with zonal wavenumber s = 4–10 and periods τ = 1–5 days from the BT instability related to the stationary RW breaking.

Last but not the least, the longitudinal structure of the interhemispheric coupling is analyzed. First, the polar vortex largely shifted to a lower latitude around 340 °E and 70 °N associated with the development of the Aleutian high, and the southwestern edge of the polar vortex is collapsed. The latitudinal gradient of angular momentum becomes small over 150 °E–340 °E. A strong meridional flow anomaly is formed in the longitude region, which leads to a strong cold anomaly at 290 °E–350 °E in the equatorial stratosphere.

In the SH mesosphere, the occurrence frequency of shear instability increases in a longitude region of ~-60 °E–~60 °E, where the parameterized GW forcing anomaly is observed. More GWs propagating upward and westward are radiated from the shear instability area. Therefore, likely due to the westward propagation of the GWs from the shear instability and their breaking in the lower thermosphere, the warm anomaly at SH high latitudes in the lower thermosphere appeared to the west of the cold anomaly in the equatorial stratosphere. The negative latitudinal gradient of potential vorticity, which is a necessary condition of BT/BC instability, is enhanced over 80 °E–200 °E. In addition, an anomaly of QTDW activity is positive in the same longitude region. These longitudinal characteristics are consistent with the scenario obtained from the analysis of the zonal mean field in this study.

Many previous studies considered that interhemispheric coupling is caused mainly by waves originated from the troposphere. However, the mechanism revealed by this study indicates that waves generated in the middle atmosphere make a significant contribution to the meridional circulation, especially in specific events such as SSWs.

Because the model used in this study has a relatively low resolution, resolved GWs may be different from those in the real atmosphere. Therefore, it is necessary to

statistically revisit the scenario presented in this study using a GW-resolving model. Moreover, it is necessary to analyze the stationary wave development observed in the SH stratosphere during the cold equatorial stratosphere events in the future since the stationary waves modulate the parameterized GW forcing and make its longitudinal structure in the SH stratosphere. Furthermore, it is recently suggested that there is a correlation between the tropospheric Arctic oscillation and the Antarctic oscillation. This correlation could be related to the change in the zonal winds in the SH stratosphere during the cold equatorial stratosphere events shown in this study. In addition, the effect of the tidal forcing is small in the altitude region examined in this study. However, its amplitudes are large above 120 km. The tides generate an electric field in the ionosphere, which is a significant parameter of the ionized atmosphere. The waves generated in the middle atmosphere may affect the momentum and energy budget not only of the neutral atmosphere but also of the ionized atmosphere. It is necessary to study the effects of tide modulation on the ionosphere in addition to the impact of GWs, RW, and RGWs generated in the SH MLT region.

要旨

北半球冬季成層圏では、成層圏突然昇温（Stratospheric Sudden Warming; SSW）がしばしば発生する。これは、北半球成層圏において対流圏起源の定在ロスビー波の砕波に伴いラグランジュ的子午面循環が駆動され、その下降（上昇）流域で断熱圧縮（膨張）により北極（赤道）成層圏が昇温（降温）する現象である。一方、南半球中間圏及び下部熱圏（MLT）では、北極 SSW 後に高温偏差が現れることが衛星観測や数値シミュレーションによって示され、SSW に伴う重力波強制による中間圏の子午面循環の変化によって南北半球間が結合するシナリオが提唱された。しかし、SSW に伴い赤道を越えて南半球低緯度成層圏まで低温偏差が形成されることや SSW 時に夏半球中間圏で準 2 日波が発達して夏半球上部中間圏に昇温をもたらすことも指摘されており、このシナリオは完全ではない可能性がある。さらに近年では、対流圏起源の重力波の強制によってもたらされる冬半球中間圏の順圧・傾圧不安定によりロスビー波が発生することや、夏半球中間圏のジェット上部でのシア不安定により重力波が 2 次的に放射されることが示されている。このような中間圏で発生するロスビー波や重力波は、気候場において中間圏及び下部熱圏の運動量収支において大きな寄与をもたらしうる。したがって、本研究では、成層圏に及ぶ大きな低温偏差をもたらすイベントに着目し、対流圏起源の重力波・ロスビー波だけでなく、中層大気で発生する重力波、ロスビー波及びロスビー重力波に伴う波強制も含めて南北半球間結合を見直し、北半球 SSW に伴って生じる南半球中間圏及び下部熱圏の気温偏差形成の要因を解明することである。

本研究では、中層大気-電離大気結合モデル Ground–to–topside model of Atmosphere and Ionosphere for Aeronomy （GAIA）による現実大気再現実験の中性大気データを用いた。モデルの解像度は T42L150 で、対流圏起源の地形性及

び非地形性重力波を表現するパラメタリゼーションが用いられている。また、地表から高度約 30 km までは Japanese 25-year Reanalysis（JRA-25）/Japan Meteorological Agency Climate Data Assimilation System（JCDAS）を用いてナッジングを行なっている。解析期間は、1996 年 12 月から 2015 年 3 月における冬から春（DJFM）の 19 シーズンである。解析高度は地表から高度 120 km までである。また、モデルシミュレーションの再現性を確認や成層圏の解析のために、それぞれ Aura Microwave Limb Sounder（MLS）観測データ及び Modern-Era Retrospective analysis for Research and Applications, Version 2（MERRA-2）を補助的に用いた。解析は、まず気候平均からの偏差を求めた後、太陽活動 11 年周期に伴う変化を取り除くために、さらに 90 日の移動平均を除去したもの（以下、簡単に「偏差」と呼ぶ）に対して行なった。着目する大きな赤道低温偏差イベントは、5 hPa における赤道及び 20 °S の気温偏差が 2 σ 以上低くなる期間として抽出し、気温偏差の最も低くなる日を中心日（Day＝0）とした。得られた全 18 事例について、気温、風、渦位、波活動度、波強制の偏差に対して各種コンポジット解析を行なった。また、各波強制の影響を調べるために、各物理量の擾乱成分のうち、潮汐波として東西波数 1~3 の成分、解像される重力波成分として周期 24 時間以下の成分、ロスビー波及びロスビー重力波として周期 24 時間より長い成分をそれぞれフーリエ解析によって抽出した。

はじめに東西平均した気温及び風の場と波活動度及び波強制の解析を行なった。赤道低温偏差イベントは、40 °S 付近まで広がる大きな成層圏低温偏差であり、北半球成層圏での大きな波強制に伴って現れることがわかった。この赤道を中心とする成層圏低温偏差が生じると、まず南半球下部熱圏に高温偏差が現れる（Day = +4）。その後、時間とともに、高温偏差域が南半球上部中間圏まで下降する様子が見られる（Day = +9）。この南半球中間圏及び下部熱圏の高温偏差

域を各波強制の偏差と比較したところ、それぞれ下部熱圏及び上部中間圏の高温偏差は、それぞれ解像される重力波、ロスビー波・ロスビー重力波による波強制によって形成されており、特に後者は主に準 2 日波（主に東西波数 3 のロスビー重力波）の寄与であることがわかった。したがって、この南北半球間結合は先行研究で提唱されたシナリオとは異なり、重力波と準 2 日波の両方の波強制の働きで生じていることがわかる。さらにこのイベントにおいて強化される準 2 日波及び重力波の一部はそれぞれ中間圏の順圧・傾圧不安定、シア不安定から発生していることも明らかになった。また、これらの順圧・傾圧不安定やシア不安定は、パラメタリゼーションで表現される対流圏起源の重力波強制によって生じている。このうちシア不安定の強化は、赤道成層圏の低温偏差に伴う東風強化が要因の一つと考えられる。

先行研究では、衛星観測や数値モデルの結果から北半球成層圏の気温偏差または波強制偏差と南半球中間圏及び下部熱圏の気温偏差の間に幅広い応答時間差（5~10 日）ことを示している。本研究で明らかとなった南半球下部熱圏と上部中間圏の高温偏差の極大日には、平均で 5 日程度の長い時間ラグがあり、先行研究と整合的である。このラグは、重力波の発生から伝播までの時間（約 1 日）と比較して、準 2 日波が中間圏で発達し上部中間圏まで伝播する時間が長いために生じていると考えられる。また、準 2 日波の発達率の季節性が大きく、12 月前半や 2 月後半には準 2 日波が見られなくなることが知られている。すなわち、幅広い応答時間は、このように性質の異なる 2 つの波が南北半球間結合に寄与していることが要因であろうと推察される。

次に、赤道成層圏に大きな低温偏差が形成されるイベントと小さな低温偏差が形成されるイベントを比較することで、南半球成層圏及び中間圏の東風偏差形成に重要な赤道成層圏低温偏差形成の要因を解析した。大きな低温偏差が現

れるイベントでは、北半球低緯度まで大きな波強制が与えられていることがわかった。特に 30 °N より低緯度では、下層から伝播する東西波数 1 のロスビー波が砕波することによって、東西波数 4~10・周期 1~5 日程度の幅広い東西波数・周波数のロスビー波が新たに発生し、より低緯度に波強制をもたらすことがわかった。

最後に、一連の南北半球間結合過程における各偏差の経度構造についても解析を行なった。まず、成層圏ではアリューシャン高気圧の振幅増大により極渦が 0 °E 付近にシフトしていた。また、その極渦の端が、270 °E 付近で崩れており、その経度での角運動量勾配が小さくなっていた。ここに形成される南北循環が、この経度帯で大きな赤道成層圏低温偏差をもたらしていた。

南半球中間圏では、シア不安定発生頻度は対流圏起源の重力波強制偏差が現れる経度帯に対応する、-60 °E~60 °E 付近で増加していた。そして、そこから西向き伝播重力波が上方に放射されるため、南極下部熱圏の高温偏差が赤道成層圏低温偏差よりも西側に位置することがわかった。一方、順圧・傾圧不安定を示す負の渦位の南北勾配偏差は 80 °E~200 °E 付近で強化されており、そこで準 2 日波の活動が高くなっていることがわかった。このように場と波の分布には、東西非一様性があるが、各経度領域での特徴は東西平均場の解析で得たシナリオと整合的であることが確認できた。

今までの南北半球間結合は、主に下層大気からやってくる大気波動が駆動していると考えられてきたが、本研究で明らかとなった南北半球間結合のシナリオは、特に SSW のような特定のイベントにおいては、中層大気中で発生する大気波動の寄与が、大きいことを指摘するものであり、これまでの描像を大きく書きかえるものである。

本研究で用いたモデルは、比較的粗い解像度であるため、重力波が歪められた

形で再現されている可能性がある。したがって、今後は重力波解像モデルを用いて、本研究で示したシナリオの統計解析を行なう必要がある。また、南北半球間結合時に見られた南半球成層圏の定在ロスビー波の発達についても解析を行なう必要がある。さらに最近、対流圏の北極振動と南極振動の間に相関があると言われている。そのような相関の発生要因として、本研究で示した成層圏東西風の変化の影響もあるかもしれない。

本研究で示した高度では、潮汐波の波強制の影響は小さかったが、高度 120 km 以上では潮汐波の振幅が大きく変わっていた。電離圏では潮汐波によって電離大気の主要なパラメータである電場が生成される。また、中層大気中で発生する大気波動は、中性大気にはとどまらず、電離圏の運動量・エネルギー収支にも影響を与える可能性がある。今後、本研究で調べた南半球中間圏及び下部熱圏で生じた重力波、ロスビー波及びロスビー重力波の電離大気への影響に加えて、潮汐波の変調による電離大気への影響の研究なども進める必要があると考えられる。

Contents

Chapter 1.
General introduction

1.1. The temperature structure of the middle atmosphere

The temperature structure of the middle atmosphere is quite different from that expected from radiative equilibrium (e.g., Leovy 1964; Shine 1987; Becker 2012). Figure 1.1 shows the climatology of the zonal mean temperature radiatively determined (Fig. 1.1a) and that of simulated by a general circulation model (GCM) for January (Fig. 1.1b) in the latitude–height section. In the radiatively determined state, O_3 (O_3 and O_2) heating through absorption of solar UV flux and CO_2 cooling by longwave radiation in the stratosphere (mesosphere) are mainly balanced. On the other hand, in the lower thermosphere, heating by solar ultraviolet (UV)/extreme ultraviolet (EUV) flux absorption and joule heating accompanied with high-energy particle precipitation, and cooling due to infrared radiation by CO_2, NO, and atomic oxygen are mainly balanced.

The temperature determined by radiative equilibrium is characterized by the warm summer stratosphere where solar radiation is incident, and by the cold stratospheric and mesospheric winter pole where solar radiation is no longer incident. However, it can be seen that the simulated temperature by the GCM has maxima in the stratospheric and mesospheric winter pole and the equatorial stratopause, and minimum in the vicinity of the polar summer mesopause. Such departure from the radiatively determined temperature is maintained by adiabatic heating or cooling associated with the meridional circulation driven by atmospheric waves in the middle atmosphere.

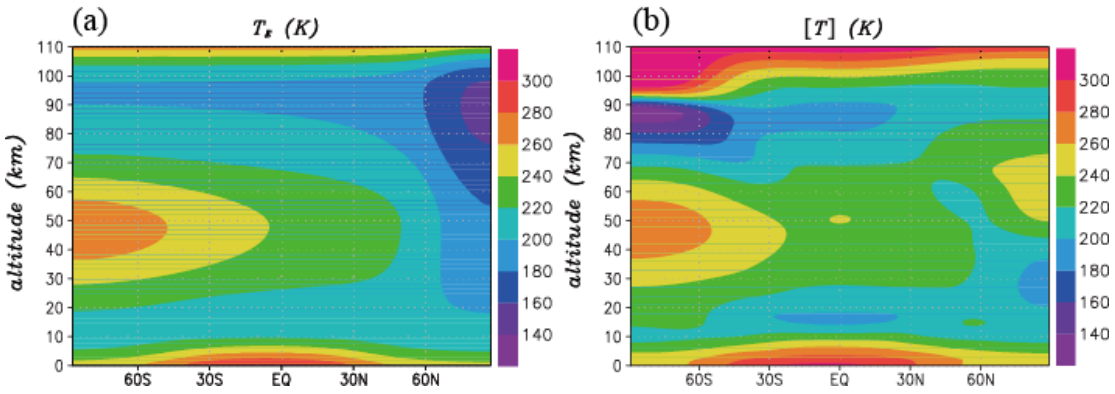

Figure 1.1: (a) The temperature determined by solar radiation and distribution of radioactive gases and (b) the temperature simulated by a GCM in January. Adapted from Becker (2012).

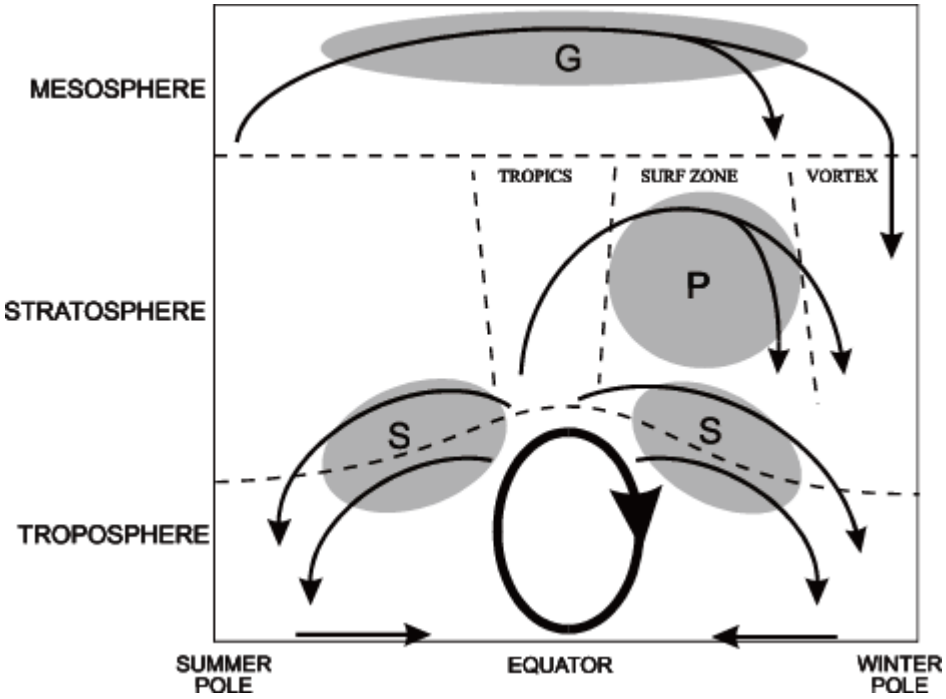

Figure 1.2: A schematic illustration of the residual mean meridional circulation in the atmosphere. The heavy ellipse denotes the thermally-driven Hadley circulation of the troposphere. The shaded regions (labeled “S”, “P”, and “G”) denote regions of breaking waves (synoptic- and planetary-scale waves, and gravity waves, respectively), responsible for driving branches of the stratospheric and mesospheric circulation. Adapted from Plumb (2002).

Figure 1.2 shows a schematic illustration of the dominant wave forcing and the residual mean meridional circulation in the lower and middle atmosphere (Plumb, 2002). The synoptic-scale Rossby waves (RWs) generated in the troposphere drive poleward flows in the subtropical upper troposphere and lower stratosphere (UTLS) in both the summer and winter hemisphere. This circulation is called shallow branches of the Brewer-Dobson circulation (BDC) (Butchart, 2014). In addition, a single poleward flow in the winter hemisphere that extends up to the middle and upper stratosphere is present and called the deep branch of the BDC (e.g., Birner and Bönisch, 2011, Butchart, 2014). The planetary-scale RWs generated by topography and land-sea temperature contrast in the troposphere deposit the westward momentum in the stratosphere and drive this deep branch of the BDC. Recently, Okamoto et al. (2011) and Sato and Hirano (2019) showed gravity wave (GW) forcing drives the summer hemispheric low latitude part of the deep branch. The difference in BDC between the summer and winter stratosphere is because that the stationary planetary-scale RWs cannot propagate due to the westward zonal wind in the summer stratosphere (Charney and Drazin, 1961). In the mesosphere, GWs originating from the troposphere break and deposit the momentum in the upper mesosphere and drive the residual mean meridional circulation from the summer pole to the winter pole.

Adiabatic heating/cooling associated with downward/upward part of the meridional circulations maintains the warm winter pole in the stratosphere and mesosphere and the cold summer pole around the mesopause. Thus, the temperatures of the summer mesopause and the winter stratopause and mesosphere in the polar region are much different from those expected from the radiative equilibrium.

1.2. Stratospheric sudden warmings (SSWs)

There is a large vortex called the “polar vortex” in the winter middle atmosphere. However, the stationary planetary-scale RWs often have a larger amplitude in the winter stratosphere and give a stronger wave forcing to the polar vortex than climatology. This wave forcing drives strong meridional circulation in the stratosphere, and the temperature in the stratospheric winter pole becomes warmer than the climatology (Matsuno, 1971). This phenomenon is called a stratospheric sudden warming (SSW). The zonal winds decelerate through the thermal wind balance with the high temperature in the winter polar region. The zonal mean zonal winds even get reversed in major SSW events. SSWs are mainly classified into the displacement type in which the polar vortex shifts from the winter pole and a split type in which the polar vortex splits into two vortices.

The mechanism of the SSW was proposed by Matsuno (1971). Using a weakly nonlinear model of the quasi-geostrophic system, it was shown that a split-type SSW appeared by forcing a stationary geopotential height disturbance with the zonal wavenumber $s = 2$ near the tropopause as is consistent with observations in 1963. This result showed that the interaction between the mean flow and planetary waves is quite essential for the SSWs. In this model, it was also seen that the polar vortex slightly shifts poleward before the SSW occurs. This phenomenon is now called preconditioning. Preconditioning occurs when the polar vortex concentrates the propagation of planetary-scale RWs in the polar stratosphere (e.g., McIntyre, 1982; Smith, 1992).

Subsequent studies showed that there is a threshold of amplitude of or wave forcing by planetary waves to generate SSWs (Holton and Mass, 1976; Sjoberg and Birner, 2014). Holton and Mass (1976) showed that the steady and vacillating modes of the zonal wind exist depending on the amplitude of the RWs in a wave-mean flow interaction model

which mimics the winter stratosphere. When the geopotential perturbations given at the tropopause, which is the lower boundary of the model, are weak, the zonal winds keep eastward. However, for the strong perturbation, the zonal winds oscillate between westward and eastward. These results showed that the zonal wind behaviors in the stratosphere are divided into two regimes depending on the RW amplitude. Recently, Yasuda et al. (2017) showed as another interpretation that the polar vortex in the winter stratosphere is in a metastable state.

1.3. Interhemispheric coupling in the middle atmosphere

The SSWs are not only the phenomena in the winter stratosphere but influence the mesosphere and thermosphere, including the ionized atmosphere (e.g., Liu and Roble, 2002; Pancheva et al., 2008; Yiğit et al., 2016). In addition, the interhemispheric coupling of the middle atmosphere, which was described by the correlation between temperature variations in the winter stratosphere and summer mesopause, was first reported by Becker et al. (2004) based on the observations of the MaCWAVE/MIDAS campaign (e.g., Goldberg et al., 2003). The interhemispheric coupling is also shown using satellite observations. Gumbel and Karlsson (2011) showed strong anti-correlation (correlation coefficient R = -0.83) between the winter stratospheric temperature anomaly from European Centre for Medium-Range Weather Forecasts (ECMWF) Interim reanalysis data and the summer mesosphere noctilucent clouds (NLCs; also known as Polar Mesospheric Clouds; PMCs) occurrence from Odins on board Optical Spectrograph and Infra-Red Imager System (OSIRIS) data. The NLCs are well observed when the temperature in the summer mesopause region is low. Thus, this result showed the correlation between the temperature in the winter stratosphere and that in the summer

mesopause region. Karlsson et al. (2009b) also showed that the PMCs occurrence frequency in the Southern Hemispheric (SH) mesosphere respond to the Northern Hemispheric (NH) zonal winds at 60 °S and 5 hPa with a delay of 2 days in December 2007 (correlation coefficient R = 0.74) and a delay of 7 days in January 2008 (correlation coefficient R = 0.91) from the Aeronomy of Ice in the Mesosphere (AIM) satellite observations.

On the other hand, many numerical simulations have been performed to show the interhemispheric coupling, and its mechanism has been proposed. Becker et al. (2004) showed using the Kühlungsborn Mechanistic general circulation model (KMCM) that an anomalous mesopause warming in the NH is caused by anomalously strong RW forcing during the stratospheric warming in austral winter 2002. Becker and Fritts (2006) showed that the enhanced winter hemisphere RW activity results in the interhemispheric coupling through a downward shift of GW-driven residual mean meridional circulation and an increased GW activity in high summer latitudes.

Moreover, Karlsson et al. (2009a) performed a composite analysis of the zonal mean temperature anomaly for respective periods with positive and negative anomalies of the vertical component of the Eliassen-Palm flux (EP-flux$_z$) in the winter stratosphere using an extended version of the Canadian Middle Atmosphere Model (CMAM). The warm (cold) anomaly in the summer mesosphere and lower thermosphere (MLT) was observed after about 10 days when positive (negative) EP-flux$_z$ anomaly in the winter stratosphere took its maximum (minimum). The positive (negative) GW drag anomaly was seen near (above) the summer mesopause for positive (negative) EP-flux$_z$ anomaly, i.e., strong (weak) planetary-scale RW events. They also hypothesized from these results that the mechanism for interhemispheric coupling is GW drag–zonal wind interaction in

the summer mesosphere. According to this hypothesis, when a positive GW forcing anomaly occurs in the summer upper mesosphere, a cold anomaly appears in its poleward side. Since the eastward wind anomaly due to thermal wind balance appears above a cold anomaly, a positive GW forcing anomaly also occurs slightly above the original level. Thus, a cold anomaly gradually shifts upward and poleward.

With these results from observations and numerical simulations, Körnich and Becker (2010) (hereafter referred to KB10) proposed the mechanism of interhemispheric coupling by the modifying the meridional circulation through the equator driven by GW forcing in the mesosphere. Figure 1.3 shows schematic illustrations of the climatological meridional circulation and the interhemispheric coupling associated with an anomalously fast deep branch of BDC caused by strong planetary wave forcing in the winter stratosphere.

This scenario argues that (1) an anomaly of the planetary-scale RW drag (δPWD) occurs in the winter stratosphere, which induces a stronger residual mean circulation than usual. This stronger meridional circulation yields the warm (cold) stratospheric winter polar region (tropics). The westward wind anomaly accompanies temperature gradient in the winter hemisphere due to a thermal wind balance. (2) More GWs with eastward phase velocity propagate into the winter mesosphere and the westward GW forcing is reduced. Thus, the GW forcing anomaly is positive (eastward) and causes the equatorward meridional circulation anomaly. This anomalous circulation forms the warm mesospheric tropics. In the summer mesosphere, the zonal wind has a positive (eastward) anomaly due to a thermal wind balance between the summer polar region and warm equatorial region in the mesosphere. (3) This positive (eastward) zonal wind anomaly in the summer mesosphere induces a downward shift of eastward GW forcing and that of meridional

circulation. Thus, the meridional circulation anomaly in the upper mesosphere is poleward and induces positive temperature anomaly at the poleward side of the negative GW forcing anomaly.

This scenario was confirmed by using an axisymmetric version of the KMCM with GW parameterizations. However, it seems that the altitude of the warm anomaly in the SH MLT region of the real atmosphere is lower than that simulated by GCMs and that the response time lag simulated by the model (~4 days) is shorter than the observations (about 5–10 days, Karlsson et al., 2009a). Note that these previous studies mainly considered the GWs generated in the troposphere.

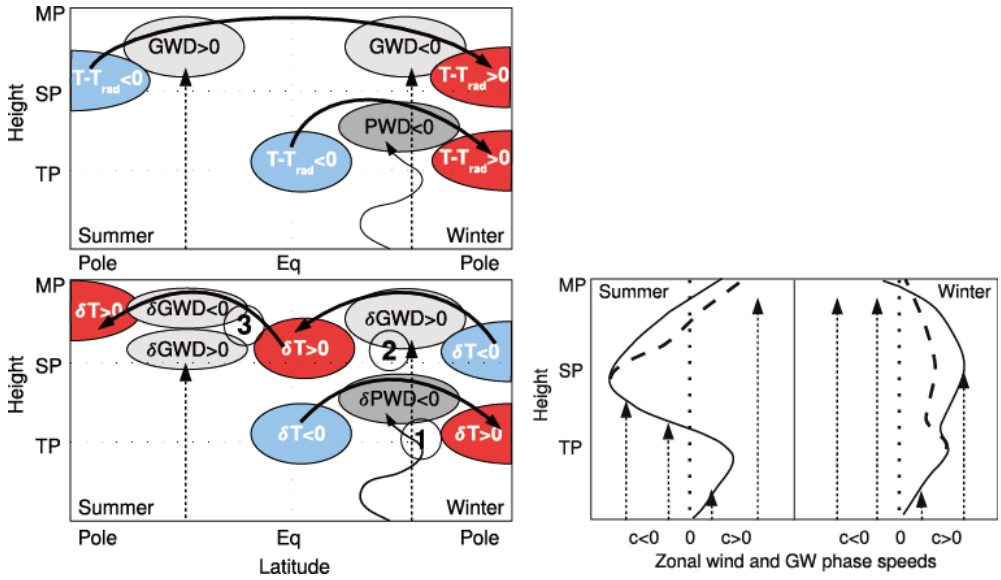

Figure 1.3: Schematic illustrations of the climatological meridional circulation (upper left panel) and of the interhemispheric coupling for a stronger Brewer–Dobson circulation in the winter stratosphere, where T, T_{rad}, GWD, and PWD denote the temperature, the radiative equilibrium temperature, the GW drag, and the planetary wave drag, respectively. In the lower left panel, the δ-symbol indicates the variable's anomaly during the stronger Brewer–Dobson circulation in comparison with the mean state. In the lower right panel, a schematic illustration of the zonal-mean wind structure and its impact on the GW propagation for the climatology (solid) and the weak winter polar vortex case (dashed). The straight dashed lines represent vertically propagating GWs with negative and positive zonal phase velocity c. The

height regions are marked by the tropopause (TP), stratopause (SP), and mesopause (MP). Adapted from Körnich and Becker (2010).

1.4 Rossby wave, Rossby-gravity wave, and gravity wave generation in the middle atmosphere

As mentioned before, the residual mean meridional circulation of the middle atmosphere has been considered driven mainly by waves originating from the troposphere. However, it has recently been shown that the momentum deposition due to waves generated in the middle atmosphere is significantly important in the MLT region. (e.g., McLandress et al., 2006; Sato and Nomoto, 2015; Becker and Vadas, 2018). Most remarkable waves in the summer MLT region are quasi 2-day waves (QTDWs), which propagate westward and have zonal wavenumber of s = 2–4 and wave periods of 40–60 h (e.g., Ern et al. 2013). The amplitude of QTDWs with s = 3 is larger than that of QTDWs with s = 2 or s = 4. The QTDWs were often observed by satellites (e.g., Rodgers and Prata, 1981; Burks and Leovy 1986; Wu et al. 1993; Wu et al., 1996; Lieberman, 1999; Lieberman, 2002; Limpasuvan and Wu, 2003; Garcia et al., 2005; Baumgaertner et al., 2008; Li et al. 2008; Tunbridge et al. 2011; Ern et al., 2013; Gu et al., 2013; Pancheva et al., 2018) and by radars such as meteor radars (e.g., Muller and Nelson, 1978; Salby and Roper, 1980; Lima et al. 2004; Pancheva et al. 2004) and medium frequency (MF) radars (e.g., Herman et al. 1999; Thayaparan et al. 1999; Pancheva et al. 2004; Murphy et al., 2007).

The QTDWs are identified as Rossby-gravity normal mode with $(s,\ n-s)$ = (3, 0), where $n-s$ represents the number of meridional nodes, (e.g., Salby, 1981a; Salby, 1981b; Salby and Callaghan, 2001; Rojas and Norton, 2007) and their seasonality explained by barotropic (BT)/baroclinic (BC) instability of the summer westward jet (e.g.,

Plumb, 1983; Pfister, 1985). Note that the Rossby-gravity waves (RGWs) are well known as equatorial waves. In terms of the normal mode, the equatorial waves can be regarded as asymptotic modes to equivalent depth $h \to 0$, i.e., vertical wavelength $\lambda_z \to 0$. Since the equatorial deformation radius is proportional to h, these modes become confined near the equator. On the other hand, the QTDWs observed in the low and mid-latitudes in the MLT region have a large h (~8 km) and λ_z (~40 km). Thus, the QTDWs have a global structure extending a wide latitude region.

Sato, Yasui, and Miyoshi (2018) (hereafter referred to SYM18) showed using Ground-to-Topside Model of Atmosphere and Ionosphere for Aeronomy (GAIA) (Jin et al., 2011) that QTDWs play a second largest role after the GWs in the momentum budget in the summer MLT region. Figure 1.4a shows latitude–height section of EP flux and its divergence (EPFD) of RWs and RGWs in January climatology (SYM18). While negative (westward) EPFD is seen in the winter stratosphere, EPFD is positive (~+10 $ms^{-1}d^{-1}$) in the summer mesosphere and negative (~-20 $ms^{-1}d^{-1}$) above. QTDWs are responsible for most of the wave forcing in the summer mesosphere. In addition, the cause of QTDWs was investigated by potential vorticity (PV) analysis. Figure 1.4b shows a latitude–potential temperature section of climatology of latitudinal gradient of modified PV (MPV; Lait, 1994) for January. The presence of negative latitudinal gradient of MPV is a necessary condition of BT/BC instability, which is observed in GAIA. Comparing Figs. 1.4a and 1.4b, the region of positive EPFD corresponds to that of negative MPV latitudinal gradient in the summer mesosphere. This means that the QTDWs are in-situ generated by BT/BC instability in the summer mesosphere. Moreover, SYM18 also showed that this BT/BC instability is caused by GW forcing. This indicates that the interplay of GWs and RGWs is important in the summer mesosphere.

It was reported that the QTDWs in the summer MLT region are amplified when the SSWs occur in the winter stratosphere (Pancheva et al., 2016; Gu et al., 2018; France et al. 2018). France et al. (2018) showed using re-analysis data from the Navy Global Environmental Model (NAVGEM) (Eckermann et al., 2018) that the BC instability is enhanced by strengthened westward jet in the summer stratosphere and mesosphere during the SSW. The forcing of the developed QTDWs weakens equatorward meridional circulation and causes a warm anomaly around the polar summer mesopause.

There are also other RWs called the 4-day waves which are generated in the winter MLT region. Venne and Stanford (1979) first reported the 4-day waves observed by the Nimbus 5 selective chopper radiometer in the winter stratosphere. By the spectral analysis of geopotential height from Nimbus 6 sounding data, Lawrence and Randel (1996) showed the existence of waves that have a zonal wavenumber s = 1 and a wave period τ ~ 4 days at 0.4 hPa (~55 km) and 72 °S in the winter. Garcia et al. (2005) also showed based on the spectral analysis of temperature data from the Sounding of the Atmosphere using Broadband Emission Radiometry (SABER) satellite instrument that s = 1 eastward waves with τ = 4.3 days are dominant poleward of 40 °N in the winter upper stratosphere and mesosphere. The 4-day waves also provide significant wave forcing in the winter MLT region. As seen in Fig. 1.4a, the EPFD reaches ~-10 $ms^{-1}d^{-1}$ in the winter MLT region in the GAIA January climatology. The 4-day waves are also considered to be generated likely due to the BT/BC instability in the winter mesosphere (see Fig. 1.4b) caused by GW forcing (Watanabe et al., 2009; Sato and Nomoto, 2015).

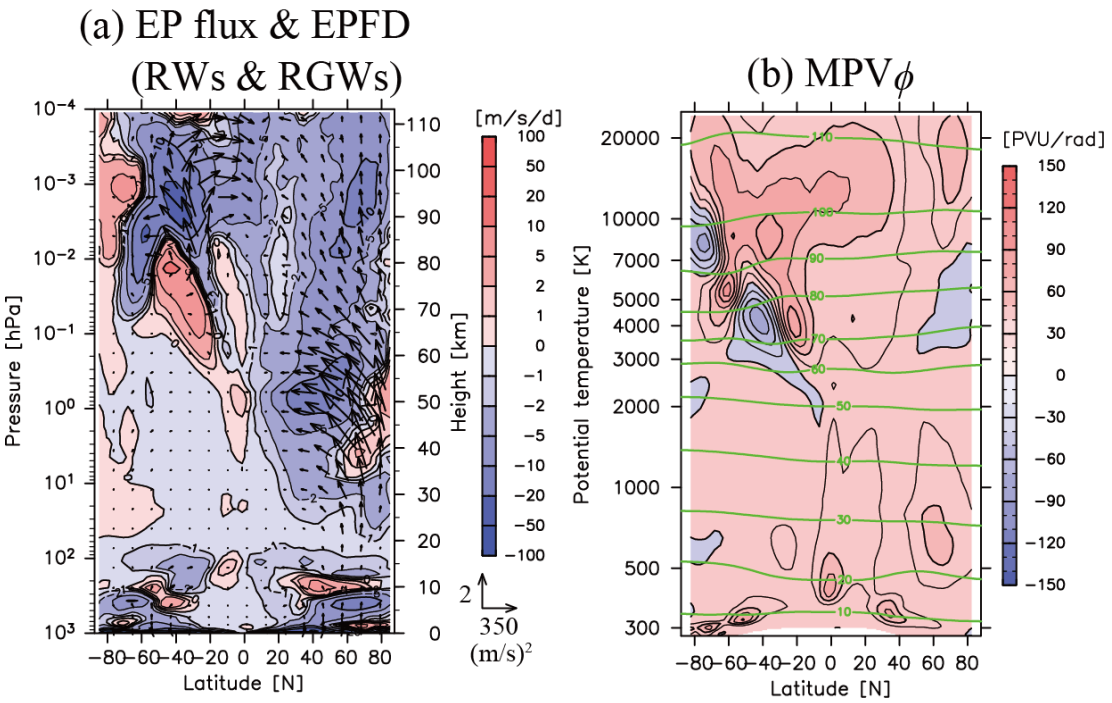

Figure 1.4: (a) Latitude–height section of Eliassen-Palm flux (EP flux) and its divergence (EPFD) of RWs and RGWs for climatology in January. Arrows denote EP flux (m^2s^{-2}). Note that the contour intervals are not uniform. (b) Latitude–potential temperature section of climatology of latitudinal gradient of MPV for January. Potential temperature is used for the vertical axis. The contour interval of MPV_{ϕ} is 15 $PVUrad^{-1}$. Green curves show contours of the geopotential height at an interval of 10 km. Adapted from SYM18.

In addition to the summer mesospheric QTDWs, it is shown that the forcing due to secondary GWs in the mesosphere is also significant (e.g., Becker and Vadas, 2018; Yasui, Sato, and Miyoshi, 2018 (YSM18)). Primary GWs mainly originate from the troposphere. Their sources are topography, convection, jet-frontal system, and wind shear (e.g., Frrits and Alexander, 2003; Yasuda et al., 2015a; Yasuda et al., 2015b; Plougonven and Zhang, 2014; Bühler et al., 1999; Bühler and McIntyre, 1999). In contrast, the secondary GWs are generated by strong body force and imbalance caused by breaking primary waves (Vadas et al., 2003; Satomura and Sato, 1999) or shear instability

(YSM18) in the MLT region. Becker and Vadas (2018) showed that primary orographic GW forcing generates the secondary GWs in the winter mesosphere using the high-resolution KMCM. These secondary GWs can propagate into the lower thermosphere and break in the high latitudes of the winter hemisphere.

Figures 1.5a, 1.5b. and, 1.5c show the latitude–height sections of January climatology of the EP flux and EPFD associated with resolved GWs, resolved GWs propagating eastward, and resolved GWs propagating westward simulated by GAIA (SYM18 and YSM18). The EPFD associated with GWs propagating westward is positive in the summer mesosphere, and the EP flux is upward in the summer MLT region. The westward propagating GWs generated in the troposphere are considered difficult to reach these altitudes. This is because the zonal winds are westward in the summer stratosphere and mesosphere and there are critical levels for the westward propagating GWs. Thus, the westward propagating resolved GWs in the summer mesosphere must be in-situ generated.

YSM18 also showed the mechanism of the GW generation in the summer MLT region. Figure 1.5d shows the latitude–height section of the occurrence frequency of Richardson number $Ri < 1/4$ (YSM18). In the summer MLT region, the occurrence frequency of $Ri < 1/4$ reaches ~8 %, and the location of positive EPFD maximum associated with westward propagating GWs corresponds well to that of the occurrence frequency of $Ri < 1/4$. Thus, the GWs propagating westward are likely generated from shear instability in the MLT region. Moreover, YSM18 also showed that shear instability is likely formed by primary GW forcing. The secondary GWs generated in the MLT region can propagate up to the thermosphere and deposit the momentum (Vadas and Crowley, 2010; Vadas and Liu, 2009; Becker and Vadas, 2018).

For these reasons, GWs generated in the MLT region may contribute to the

formation of a warm anomaly in the summer MLT region similar to QTDWs. In addition, the generation mechanisms of QTDWs during an SSW have not been examined in detail. Furthermore, previous studies discussed only interhemispheric coupling in terms of zonal mean fields. There are no previous studies regarding the longitudinal structure of interhemispheric coupling.

The purpose of this thesis is to elucidate the formation mechanisms of interhemispheric coupling in the SH MLT region associated with the NH SSWs including wave forcings due to the RWs, RGWs, and GWs generated in the middle atmosphere. The longitudinal structure of the interhemispheric coupling is also examined.

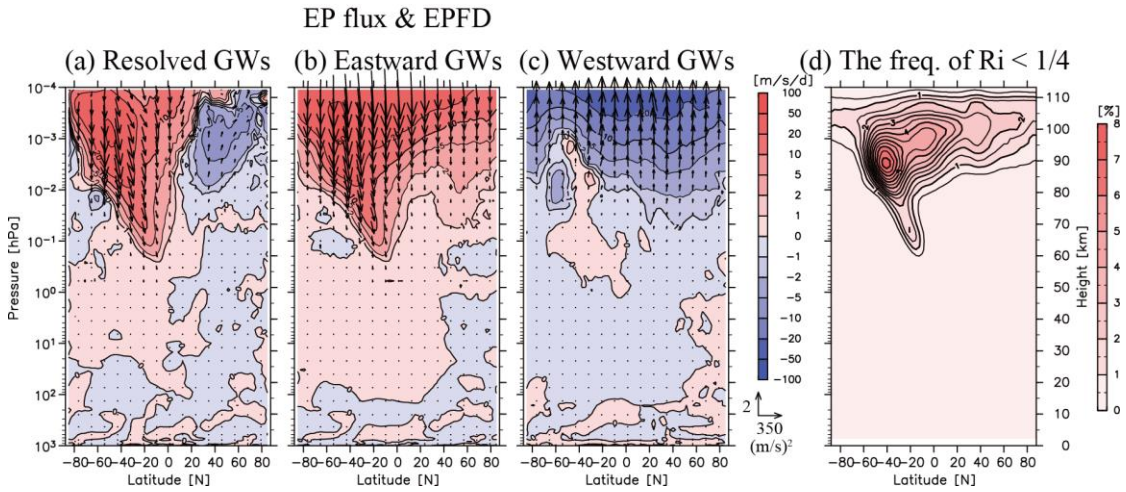

Figure 1.5: Latitude–height sections of Eliassen-Palm flux (EP flux) and its divergence (EPFD) of (a) resolved GWs, (b) resolved GWs propagating eastward, and (c) resolved GWs propagating westward for climatology in January. Arrows denote EP flux (m^2s^{-2}). Note that the contour intervals are not uniform. (d) Latitude–height sections of the occurrence frequencies of Ri < 1/4 during January obtained from the GAIA simulation data. The contour interval is 0.5%. Adapted from SYM18 and YSM18.

1.5 Overview of this thesis

In this study, the temperature structure and mechanisms of interhemispheric coupling in boreal winter, including the effects of wave forcing generated in the MLT region, are examined using data from GAIA, which is a whole atmosphere model. Aura MLS observations and MERRA-2 re-analysis data are also used for the model validation and analysis for the stratosphere. The events when a large cold anomaly appears in the equatorial upper stratosphere which is mainly associated with SSWs in the NH are focused, and the results of the composite analysis are shown. In the SH, a warm anomaly is first observed in the high latitudes of the lower thermosphere during the cold equatorial stratosphere events. A warm anomaly is formed in the upper mesosphere about 5 days after that in the lower thermosphere. The downward and equatorward shift of a warm anomaly of the summer MLT region is first shown in this study.

Next, the wave forcing anomaly is examined. In the summer MLT region, positive (negative) anomaly of resolved GW forcing is seen in the upper mesosphere (lower thermosphere). Furthermore, a pair of positive and negative anomalies of QTDW forcing is observed in the summer mesosphere. These results suggest that GWs and QTDWs are in-situ generated. These GWs and the QTDWs are likely radiated from the shear instability and the BT/BC instability in the summer mesosphere, respectively. It is also shown that these instabilities are formed by the enhanced westward wind related to the thermal wind balance and parameterized GW forcing anomaly of the summer stratosphere and mesosphere.

The causes of the formation of the cold anomaly in the equatorial stratosphere, where the westward wind anomaly balances by the thermal wind relation in the SH stratosphere and mesosphere, are examined. It is shown that a cold anomaly of equatorial

stratosphere appears when a negative RW forcing in the stratosphere is seen not only in the mid- and high latitudes but also in the low latitudes. The RW generation in the NH upper stratosphere is important for the existence of the negative RW forcing in low latitudes.

Finally, the longitudinal structure of interhemispheric coupling is analyzed. The warm anomaly in the SH lower thermosphere is located westward of the cold anomaly in the equatorial stratosphere. This is caused by westward propagating GWs from the shear instability. These results in the present study indicate that GW and QTDW generation in the MLT region is significant for the interhemispheric coupling, in addition to GW originating from the troposphere considered in previous studies.

The thesis is organized as follows. The descriptions of the data from GAIA, Aura MLS, and MERRA-2 used in this study and the methods of analyses are given in Chapter 2. Chapter 3 shows the zonal mean temperature anomaly and zonal mean wave forcing anomaly of each wave type which are crucial to the interhemispheric coupling. The causes of the wave forcing anomaly are also analyzed in this Chapter. Chapter 4 shows the results of the longitudinal structure of the interhemispheric coupling phenomena and its mechanisms. Summary and concluding remarks are given in Chapter 5.

Chapter 2.
Data and analysis methods

In this study, three kinds of data are used for the analyses of interhemispheric coupling. They are model simulation, satellite observation, and re-analysis data. The model data is mainly analyzed from the ground to the MLT region, and the satellite observation data and the re-analysis data are used to validate the model simulation and confirm results of the analysis in the stratosphere and mesosphere.

本章については、5 年以内に雑誌等で刊行予定のため、以降の節について、非公開。

Chapter 3.
Composite analysis of zonal mean fields regarding the interhemispheric coupling

In this chapter, characteristics of the zonal mean fields for the interhemispheric coupling are shown. Since various waves are considered to play important roles in the interhemispheric coupling, changes in each wave forcing and its mechanism are examined. The results are discussed and compared with the KB10 scenario. In Section 3.1, time evolution of the interhemispheric coupling simulated by GAIA is described. Sections 3.2 and 3.3 discuss plausible mechanisms of resolved GW and QTDW forcing anomalies related to the interhemispheric coupling. Section 3.4 newly proposes a mechanism how the anomalous cold equatorial stratosphere events affect the interhemispheric coupling. Section 3.5 examines the causes of the anomalous cold equatorial stratosphere events.

本章については、5 年以内に雑誌等で刊行予定のため、以降の節について、非公開。

Chapter 4.
Composite analysis for the longitudinal structure of interhemispheric coupling

Many previous studies for the interhemispheric coupling have focused on the zonal mean fields and have not analyzed its longitudinal structure. However, the longitudinal structure of temperature anomaly related to the interhemispheric coupling can significantly influence the thermosphere as well as the ionosphere where characteristics have strong local time dependence owing to the solar radiation. In this chapter, the longitudinal structure of temperature anomaly associated with the cold equatorial stratosphere events is analyzed. The results will reinforce the interhemispheric coupling scenario obtained from the analysis of the zonal mean fields in the previous chapter.

本章については、5 年以内に雑誌等で刊行予定のため、以降の節について、非公開。

Chapter 5.
Summary and concluding remarks

本章については、5 年以内に雑誌等で刊行予定のため、非公開。

Acknowledgements

I would particularly like to express my gratitude to my supervisor Prof. Kaoru Sato. I also thank Profs. Yu Kosaka, Hiroyasu Hasumi, Toshihiko Hirooka, and Keita Iga for their many useful comments and discussions. I also thank Profs. Yasunobu Miyoshi at Kyushu University and Hitoshi Fujiwara at Seikei University, and Dr. Hiroyuki Shinagawa, Dr. Hidekatsu Jin, and Dr. Chihiro Tao at National Institute of Information and Communications Technology (NICT) for their useful comments and discussions. Special thanks are given to colleagues and former members in the atmospheric dynamics laboratory: Dr. Masashi Kohma, Dr. Yukari Sumi, Dr. Maria Mihalikova, Dr. Kota Okamoto, Mr. Masahiro Nomoto, Dr. Yuki Yasuda, Dr. Ryosuke Shibuya, Dr. Arata Amemiya, Dr. Soichiro Hirano, Mr. Yuki Hayashi, Mr. Yuichi Minamihara, Mr. Dai Koshin, Mr. Shun Nakajima, Mr. Yuki Matsushita, Ms. Haruka Okui, and Mr. Masatoshi Mizukoshi.

This study was supported by JST CREST JPMJCR1663 and JSPS KAKENHI Grant-in-Aid for JSPS Fellows JP17J07579. All figures except citations are created using the Dennou Club Library (DCL). The numerical simulation in this work was performed using the Hitachi SH16000/M1 and the NICT Science Cloud System, Japan. The Aura MLS data were obtained from EOS MLS Science Team (2011), MLS/Aura Level 2 Temperature V004 and Geopotential Height V004, Greenbelt, MD, USA, Goddard Earth Sciences Data and Information Services Center (GES-DISC), Accessed: April 2018, https://acdisc.gesdisc.eosdis.nasa.gov/data/Aura_MLS_Level2/ML2T.004 and https://acdisc.gesdisc.eosdis.nasa.gov/data/Aura_MLS_Level2/ML2GPH.004. The MERRA-2 data were provided by Global Modeling and Assimilation Office (GMAO) (2015), MERRA-2 inst3_3d_asm_Np: 3d,3-Hourly,Instantaneous,Pressure-

Level,Assimilation,Assimilated Meteorological Fields V5.12.4, Greenbelt, MD, USA, Goddard Earth Sciences Data and Information Services Center (GES DISC), Accessed: February 2018, 10.5067/QBZ6MG944HW0.

References

Andrews, D. G., J. R. Holton, and C. B. Leovy, 1987: *Middle Atmosphere Dynamics*. Academic Press.

Baumgaertner, A. J. G., A. J. McDonald, R. E. Hibbins, D. C. Fritts, D. J. Murphy, and R. A. Vincent, 2008: Short-period planetary waves in the Antarctic middle atmosphere. *Journal of Atmospheric and Solar-Terrestrial Physics*, **70**, 1336–1350, https://doi.org/10.1016/j.jastp.2008.04.007.

Becker, E., 2004: High Rossby-wave activity in austral winter 2002: Modulation of the general circulation of the MLT during the MaCWAVE/MIDAS northern summer program. *Geophysical Research Letters*, **31**, L24S03, https://doi.org/10.1029/2004GL019615.

Becker, E., 2012: Dynamical Control of the Middle Atmosphere. *Space Science Reviews*, **168**, 283–314, https://doi.org/10.1007/s11214-011-9841-5.

Becker, E., and D. C. Fritts, 2006: Enhanced gravity-wave activity and interhemispheric coupling during the MaCWAVE/MIDAS northern summer program 2002. *Annales Geophysicae*, **24**, 1175–1188, https://doi.org/10.5194/angeo-24-1175-2006.

Becker, E., and S. L. Vadas, 2018: Secondary Gravity Waves in the Winter Mesosphere: Results From a High-Resolution Global Circulation Model. *Journal of Geophysical Research: Atmospheres*, **123**, 2605–2627, https://doi.org/10.1002/2017JD027460.

Birner, T., and H. Bönisch, 2011: Residual circulation trajectories and transit times into the extratropical lowermost stratosphere. *Atmospheric Chemistry and Physics*, **11**, 817–827, https://doi.org/10.5194/acp-11-817-2011.

Bühler, O., and M. E. McIntyre, 1999: On Shear-Generated Gravity Waves that Reach the Mesosphere. Part II: Wave Propagation. *Journal of the Atmospheric Sciences*, **56**, 3764–3773, https://doi.org/10.1175/1520-0469(1999)056<3764:OSGGWT>2.0.CO;2.

——, ——, and J. F. Scinocca, 1999: On Shear-Generated Gravity Waves that Reach the

Mesosphere. Part I: Wave Generation. *Journal of the Atmospheric Sciences*, **56**, 3749–3763, https://doi.org/10.1175/1520-0469(1999)056<3749:OSGGWT>2.0.CO;2.

Burks, D., and C. Leovy, 1986: Planetary waves near the mesospheric easterly jet. *Geophysical Research Letters*, **13**, 193–196, https://doi.org/10.1029/GL013i003p00193.

Butchart, N., 2014: The Brewer-Dobson circulation. *Reviews of Geophysics*, **52**, 157–184, https://doi.org/10.1002/2013RG000448.

Charlton, A. J., and L. M. Polvani, 2007: A New Look at Stratospheric Sudden Warmings. Part I: Climatology and Modeling Benchmarks. *Journal of Climate*, **20**, 449–469, https://doi.org/10.1175/JCLI3996.1.

Charney, J. G., and P. G. Drazin, 1961: Propagation of planetary-scale disturbances from the lower into the upper atmosphere. *Journal of Geophysical Research*, **66**, 83–109, https://doi.org/10.1029/JZ066i001p00083.

Chau, J. L., B. G. Fejer, and L. P. Goncharenko, 2009: Quiet variability of equatorial **E** × **B** drifts during a sudden stratospheric warming event. *Geophysical Research Letters*, **36**, L05101, https://doi.org/10.1029/2008GL036785.

Dunkerton, T. J., 1989: Nonlinear Hadley Circulation Driven by Asymmetric Differential Heating. *Journal of the Atmospheric Sciences*, **46**, 956–974, https://doi.org/10.1175/1520-0469(1989)046<0956:NHCDBA>2.0.CO;2.

Eckermann, S. D., and Coauthors, 2018: High-Altitude (0–100 km) Global Atmospheric Reanalysis System: Description and Application to the 2014 Austral Winter of the Deep Propagating Gravity Wave Experiment (DEEPWAVE). *Monthly Weather Review*, **146**, 2639–2666, https://doi.org/10.1175/MWR-D-17-0386.1.

Ern, M., P. Preusse, S. Kalisch, M. Kaufmann, and M. Riese, 2013: Role of gravity waves in the forcing of quasi two-day waves in the mesosphere: An observational study. *Journal of Geophysical Research: Atmospheres*, **118**, 3467–3485, https://doi.org/10.1029/2012JD018208.

France, J. A., and Coauthors, 2018: Local and Remote Planetary Wave Effects on Polar Mesospheric Clouds in the Northern Hemisphere in 2014. *Journal of Geophysical*

Research: Atmospheres, **123**, 5149–5162, https://doi.org/10.1029/2017JD028224.

Fritts, D. C., and M. J. Alexander, 2003: Gravity wave dynamics and effects in the middle atmosphere. *Reviews of Geophysics*, **41(1)**, 1003, https://doi.org/10.1029/2001RG000106.

——, and ——, 2012: Correction to "Gravity wave dynamics and effects in the middle atmosphere". *Reviews of Geophysics*, **50**, RG3004, https://doi.org/10.1029/2012RG000409.

Garcia, R. R., R. Lieberman, J. M. Russell, and M. G. Mlynczak, 2005: Large-Scale Waves in the Mesosphere and Lower Thermosphere Observed by SABER. *Journal of the Atmospheric Sciences*, **62**, 4384–4399, https://doi.org/10.1175/JAS3612.1.

Garcia, R. R., D. R. Marsh, D. E. Kinnison, B. A. Boville, and F. Sassi, 2007: Simulation of secular trends in the middle atmosphere, 1950–2003. *Journal of Geophysical Research*, **112**, D09301, https://doi.org/10.1029/2006JD007485.

Gelaro, R., and Coauthors, 2017: The Modern-Era Retrospective Analysis for Research and Applications, Version 2 (MERRA-2). *Journal of Climate*, **30**, 5419–5454, https://doi.org/10.1175/JCLI-D-16-0758.1.

Goldberg, R. A., 2004: The MaCWAVE/MIDAS rocket and ground-based measurements of polar summer dynamics: Overview and mean state structure. *Geophysical Research Letters*, **31**, L24S02, https://doi.org/10.1029/2004GL019411.

Goncharenko, L., and S.-R. Zhang, 2008: Ionospheric signatures of sudden stratospheric warming: Ion temperature at middle latitude. *Geophysical Research Letters*, **35**, L21103, https://doi.org/10.1029/2008GL035684.

Gu, S.-Y., T. Li, X. Dou, Q. Wu, M. G. Mlynczak, and J. M. Russell, 2013: Observations of Quasi-Two-Day wave by TIMED/SABER and TIMED/TIDI. *Journal of Geophysical Research: Atmospheres*, **118**, 1624–1639, https://doi.org/10.1002/jgrd.50191.

——, X. Dou, D. Pancheva, W. Yi, and T. Chen, 2018: Investigation of the Abnormal Quasi 2-Day Wave Activities During the Sudden Stratospheric Warming Period of January 2006. *Journal of Geophysical Research: Space Physics*, **123**, 6031–

6041, https://doi.org/10.1029/2018JA025596.

Gumbel, J., and B. Karlsson, 2011: Intra- and inter-hemispheric coupling effects on the polar summer mesosphere. *Geophysical Research Letters*, **38**, L14804, https://doi.org/10.1029/2011GL047968.

Herman, R. L., W. A. Robinson, and S. J. Franke, 1999: Observational evidence of quasi two-day/gravity wave interaction using MF Radar. *Geophysical Research Letters*, **26**, 1141–1144, https://doi.org/10.1029/1999GL900157.

Hitchman, M. H., C. B. Leovy, J. C. Gille, and P. L. Bailey, 1987: Quasi-Stationary Zonally Asymmetric Circulations in the Equatorial Lower Mesosphere. *Journal of the Atmospheric Sciences*, **44**, 2219–2236, https://doi.org/10.1175/1520-0469(1987)044<2219:QSZACI>2.0.CO;2.

Holton, J. R., and C. Mass, 1976: Stratospheric Vacillation Cycles. *Journal of the Atmospheric Sciences*, **33**, 2218–2225, https://doi.org/10.1175/1520-0469(1976)033<2218:SVC>2.0.CO;2.

Inatsu, M., and B. J. Hoskins, 2004: The Zonal Asymmetry of the Southern Hemisphere Winter Storm Track. *Journal of Climate*, **17**, 4882–4892, https://doi.org/10.1175/JCLI-3232.1.

Jin, H., and Coauthors, 2011: Vertical connection from the tropospheric activities to the ionospheric longitudinal structure simulated by a new Earth's whole atmosphere-ionosphere coupled model. *Journal of Geophysical Research: Space Physics*, **116**, A01316, https://doi.org/10.1029/2010JA015925.

——, Y. Miyoshi, D. Pancheva, P. Mukhtarov, H. Fujiwara, and H. Shinagawa, 2012: Response of migrating tides to the stratospheric sudden warming in 2009 and their effects on the ionosphere studied by a whole atmosphere-ionosphere model GAIA with COSMIC and TIMED/SABER observations. *Journal of Geophysical Research: Space Physics*, **117**, A10323, https://doi.org/10.1029/2012JA017650.

Karlsson, B., C. McLandress, and T. G. Shepherd, 2009a: Inter-hemispheric mesospheric coupling in a comprehensive middle atmosphere model. *Journal of Atmospheric and Solar-Terrestrial Physics*, **71**, 518–530, https://doi.org/10.1016/j.jastp.2008.08.006.

Karlsson, B., C. E. Randall, S. Benze, M. Mills, V. L. Harvey, S. M. Bailey, and J. M. Russell III, 2009b: Intra-seasonal variability of polar mesospheric clouds due to inter-hemispheric coupling. *Geophysical Research Letters*, **36**, L20802, https://doi.org/10.1029/2009GL040348.

Kinoshita, T., and K. Sato, 2013a: A Formulation of Three-Dimensional Residual Mean Flow Applicable Both to Inertia–Gravity Waves and to Rossby Waves. *Journal of the Atmospheric Sciences*, **70**, 1577–1602, https://doi.org/10.1175/JAS-D-12-0137.1.

——, and ——, 2013b: A Formulation of Unified Three-Dimensional Wave Activity Flux of Inertia–Gravity Waves and Rossby Waves. *Journal of the Atmospheric Sciences*, **70**, 1603–1615, https://doi.org/10.1175/JAS-D-12-0138.1.

Kleist, D. T., D. F. Parrish, J. C. Derber, R. Treadon, W.-S. Wu, and S. Lord, 2009: Introduction of the GSI into the NCEP Global Data Assimilation System. *Weather and Forecasting*, **24**, 1691–1705, https://doi.org/10.1175/2009WAF2222201.1.

Körnich, H., and E. Becker, 2010: A simple model for the interhemispheric coupling of the middle atmosphere circulation. *Advances in Space Research*, **45**, 661–668, https://doi.org/10.1016/j.asr.2009.11.001.

Lait, L. R., 1994: An Alternative Form for Potential Vorticity. *Journal of the Atmospheric Sciences*, **51**, 1754–1759, https://doi.org/10.1175/1520-0469(1994)051<1754:AAFFPV>2.0.CO;2.

Lawrence, B. N., and W. J. Randel, 1996: Variability in the mesosphere observed by the Nimbus 6 pressure modulator radiometer. *Journal of Geophysical Research: Atmospheres*, **101**, 23475–23489, https://doi.org/10.1029/96JD01652.

Leovy, C., 1964: Radiative Equilibrium of the Mesosphere. *Journal of the Atmospheric Sciences*, **21**, 238–248, https://doi.org/10.1175/1520-0469(1964)021<0238:REOTM>2.0.CO;2.

Li, T., C.-Y. She, S. E. Palo, Q. Wu, H.-L. Liu, and M. L. Salby, 2008: Coordinated lidar and TIMED observations of the quasi-two-day wave during August 2002–2004 and possible quasi-biennial oscillation influence. *Advances in Space Research*, **41**, 1463–1471, https://doi.org/10.1016/j.asr.2007.03.052.

Lieberman, R. S., 1999: Eliassen–Palm Fluxes of the 2-Day Wave. *Journal of the Atmospheric Sciences*, **56**, 2846–2861, https://doi.org/10.1175/1520-0469(1999)056<2846:EPFOTD>2.0.CO;2.

——, 2002: CORRIGENDUM. *Journal of the Atmospheric Sciences*, **59**, 2625–2627, https://doi.org/10.1175/1520-0469(2002)059<2625:C>2.0.CO;2.

Lima, L. M., P. P. Batista, H. Takahashi, and B. R. Clemesha, 2004: Quasi-two-day wave observed by meteor radar at 22.7°S. *Journal of Atmospheric and Solar-Terrestrial Physics*, **66**, 529–537, https://doi.org/10.1016/j.jastp.2004.01.007.

Limpasuvan, V., 2003: Two-day wave observations of UARS Microwave Limb Sounder mesospheric water vapor and temperature. *Journal of Geophysical Research*, **108 (D10)**, 4307, https://doi.org/10.1029/2002JD002903.

Lindzen, R. S., 1981: Turbulence and stress owing to gravity wave and tidal breakdown. *Journal of Geophysical Research*, **86**, 9707–9714, https://doi.org/10.1029/JC086iC10p09707.

Liu, H.-L., and R. G. Roble, 2002: A study of a self-generated stratospheric sudden warming and its mesospheric-lower thermospheric impacts using the coupled TIME-GCM/CCM3. *Journal of Geophysical Research: Atmospheres*, **107(D23)**, 4695, https://doi.org/10.1029/2001JD001533.

——, W. Wang, A. D. Richmond, and R. G. Roble, 2010: Ionospheric variability due to planetary waves and tides for solar minimum conditions. *Journal of Geophysical Research: Space Physics*, **115**, A00G01, https://doi.org/10.1029/2009JA015188.

Matsuno, T., 1971: A Dynamical Model of the Stratospheric Sudden Warming. *Journal of the Atmospheric Sciences*, **28**, 1479–1494, https://doi.org/10.1175/1520-0469(1971)028<1479:ADMOTS>2.0.CO;2.

McCormack, J. P., L. Coy, and K. W. Hoppel, 2009: Evolution of the quasi 2-day wave during January 2006. *Journal of Geophysical Research*, **114**, D20115, https://doi.org/10.1029/2009JD012239.

McFarlane, N. A., 1987: The Effect of Orographically Excited Gravity Wave Drag on the General Circulation of the Lower Stratosphere and Troposphere. *Journal of the Atmospheric Sciences*, **44**, 1775–1800, https://doi.org/10.1175/1520-

0469(1987)044<1775:TEOOEG>2.0.CO;2.

McIntyre, M. E., 1982: How Well do we Understand the Dynamics of Stratospheric Warmings? *Journal of the Meteorological Society of Japan. Ser. II*, **60**, 37–65, https://doi.org/10.2151/jmsj1965.60.1_37.

McLandress, C., W. E. Ward, V. I. Fomichev, K. Semeniuk, S. R. Beagley, N. A. McFarlane, and T. G. Shepherd, 2006: Large-scale dynamics of the mesosphere and lower thermosphere: An analysis using the extended Canadian Middle Atmosphere Model. *Journal of Geophysical Research*, **111**, D17111, https://doi.org/10.1029/2005JD006776.

Medvedeva, I. V., A. I. Semenov, V. I. Perminov, A. B. Beletsky, and A. V. Tatarnikov, 2014: Comparison of ground-based OH temperature data measured at Irkutsk (52°N, 103°E) and Zvenigorod (56°N, 37°E) stations with Aura MLS v3.3. *Acta Geophysica*, **62**, 340–349, https://doi.org/10.2478/s11600-013-0161-x.

Miyoshi, Y., and H. Fujiwara, 2003: Day-to-day variations of migrating diurnal tide simulated by a GCM from the ground surface to the exobase. *Geophysical Research Letters*, **30(15)**, 1789, https://doi.org/10.1029/2003GL017695.

——, ——, H. Jin, and H. Shinagawa, 2014: A global view of gravity waves in the thermosphere simulated by a general circulation model. *Journal of Geophysical Research: Space Physics*, **119**, 5807–5820, https://doi.org/10.1002/2014JA019848.

——, ——, ——, and ——, 2015: Impacts of sudden stratospheric warming on general circulation of the thermosphere. *Journal of Geophysical Research: Space Physics*, **120**, 10,897–10,912, https://doi.org/10.1002/2015JA021894.

Mlynczak, M. G., C. J. Mertens, R. R. Garcia, and R. W. Portmann, 1999: A detailed evaluation of the stratospheric heat budget: 2. Global radiation balance and diabatic circulations. *Journal of Geophysical Research: Atmospheres*, **104**, 6039–6066, https://doi.org/10.1029/1998JD200099.

Molod, A., L. Takacs, M. Suarez, and J. Bacmeister, 2015: Development of the GEOS-5 atmospheric general circulation model: evolution from MERRA to MERRA2. *Geoscientific Model Development*, **8**, 1339–1356, https://doi.org/10.5194/gmd-8-

1339-2015.

Muller, H. G., and L. Nelson, 1978: A travelling quasi 2-day wave in the meteor region. *Journal of Atmospheric and Terrestrial Physics*, **40**, 761–766, https://doi.org/10.1016/0021-9169(78)90136-8.

Murphy, D. J., W. J. R. French, and R. A. Vincent, 2007: Long-period planetary waves in the mesosphere and lower thermosphere above Davis, Antarctica. *Journal of Atmospheric and Solar-Terrestrial Physics*, **69**, 2118–2138, https://doi.org/10.1016/j.jastp.2007.06.008.

Okamoto, K., K. Sato, and H. Akiyoshi, 2011: A study on the formation and trend of the Brewer-Dobson circulation. *Journal of Geophysical Research*, **116**, D10117, https://doi.org/10.1029/2010JD014953.

Onogi, K., and Coauthors, 2007: The JRA-25 Reanalysis. *Journal of the Meteorological Society of Japan. Ser. II*, **85**, 369–432, https://doi.org/10.2151/jmsj.85.369.

Pancheva, D., and Coauthors, 2004: Variability of the quasi-2-day wave observed in the MLT region during the PSMOS campaign of June–August 1999. *Journal of Atmospheric and Solar-Terrestrial Physics*, **66**, 539–565, https://doi.org/10.1016/j.jastp.2004.01.008.

——, and Coauthors, 2008: Planetary waves in coupling the stratosphere and mesosphere during the major stratospheric warming in 2003/2004. *Journal of Geophysical Research*, **113**, D12105, https://doi.org/10.1029/2007JD009011.

Pancheva, D., P. Mukhtarov, D. E. Siskind, and A. K. Smith, 2016: Global distribution and variability of quasi 2 day waves based on the NOGAPS-ALPHA reanalysis model: QTDWs in NOGAPS-ALPHA Reanalysis Model. *Journal of Geophysical Research: Space Physics*, **121**, 11,422–11,449, https://doi.org/10.1002/2016JA023381.

——, ——, and ——, 2018: Climatology of the quasi-2-day waves observed in the MLS/Aura measurements (2005–2014). *Journal of Atmospheric and Solar-Terrestrial Physics*, **171**, 210–224, https://doi.org/10.1016/j.jastp.2017.05.002.

Pfister, L., 1985: Baroclinic Instability of Easterly Jets with Applications to the Summer Mesosphere. *Journal of the Atmospheric Sciences*, **42**, 313–330,

https://doi.org/10.1175/1520-0469(1985)042<0313:BIOEJW>2.0.CO;2.

Plougonven, R., and F. Zhang, 2014: Internal gravity waves from atmospheric jets and fronts. *Reviews of Geophysics*, **52**, 33–76, https://doi.org/10.1002/2012RG000419.

Plumb, R. A., 1983: Baroclinic Instability of the Summer Mesosphere: A Mechanism for the Quasi-Two-Day Wave? *Journal of the Atmospheric Sciences*, **40**, 262–270, https://doi.org/10.1175/1520-0469(1983)040<0262:BIOTSM>2.0.CO;2.

——, 2002: Stratospheric Transport. *Journal of the Meteorological Society of Japan. Ser. II*, **80**, 793–809, https://doi.org/10.2151/jmsj.80.793.

Randel, W. J., F. Wu, J. M. Russell, A. Roche, and J. W. Waters, 1998: Seasonal Cycles and QBO Variations in Stratospheric CH_4 and H_2O Observed in *UARS* HALOE Data. *Journal of the Atmospheric Sciences*, **55**, 163–185, https://doi.org/10.1175/1520-0469(1998)055<0163:SCAQVI>2.0.CO;2.

Richards, P. G., J. A. Fennelly, and D. G. Torr, 1994: EUVAC: A solar EUV Flux Model for aeronomic calculations. *Journal of Geophysical Research*, **99**, 8981–8992, https://doi.org/10.1029/94JA00518.

Rodgers, C. D., and A. J. Prata, 1981: Evidence for a traveling two-day wave in the middle atmosphere. *Journal of Geophysical Research*, **86**, 9661–9664, https://doi.org/10.1029/JC086iC10p09661.

Rojas, M., and W. Norton, 2007: Amplification of the 2-day wave from mutual interaction of global Rossby-gravity and local modes in the summer mesosphere. *Journal of Geophysical Research*, **112**, D12114, https://doi.org/10.1029/2006JD008084.

Sakazaki, T., K. Sato, Y. Kawatani, and S. Watanabe, 2015: Three-dimensional structures of tropical nonmigrating tides in a high-vertical-resolution general circulation model: Nonmigrating tides in a GCM. *Journal of Geophysical Research: Atmospheres*, **120**, 1759–1775, https://doi.org/10.1002/2014JD022464.

Salby, M. L., 1981a: The 2-day wave in the middle atmosphere: Observations and theory. *Journal of Geophysical Research*, **86**, 9654–9660, https://doi.org/10.1029/JC086iC10p09654.

——, 1981b: Rossby Normal Modes in Nonuniform Background Configurations. Part II. Equinox and Solstice Conditions. *Journal of the Atmospheric Sciences*, **38**, 1827–1840, https://doi.org/10.1175/1520-0469(1981)038<1827:RNMINB>2.0.CO;2.

——, and R. G. Roper, 1980: Long-Period Oscillations in the Meteor Region. *Journal of the Atmospheric Sciences*, **37**, 237–244, https://doi.org/10.1175/1520-0469(1980)037<0237:LPOITM>2.0.CO;2.

——, and P. F. Callaghan, 2001: Seasonal Amplification of the 2-Day Wave: Relationship between Normal Mode and Instability. *Journal of the Atmospheric Sciences*, **58**, 1858–1869, https://doi.org/10.1175/1520-0469(2001)058<1858:SAOTDW>2.0.CO;2.

Sato, K., and M. Nomoto, 2015: Gravity Wave–Induced Anomalous Potential Vorticity Gradient Generating Planetary Waves in the Winter Mesosphere. *Journal of the Atmospheric Sciences*, **72**, 3609–3624, https://doi.org/10.1175/JAS-D-15-0046.1.

——, and S. Hirano, 2019: The climatology of the Brewer–Dobson circulation and the contribution of gravity waves. *Atmospheric Chemistry and Physics*, **19**, 4517–4539, https://doi.org/10.5194/acp-19-4517-2019.

——, R. Yasui, and Y. Miyoshi, 2018: The Momentum Budget in the Stratosphere, Mesosphere, and Lower Thermosphere. Part I: Contributions of Different Wave Types and In Situ Generation of Rossby Waves. *Journal of the Atmospheric Sciences*, **75**, 3613–3633, https://doi.org/10.1175/JAS-D-17-0336.1.

Satomura, T., and K. Sato, 1999: Secondary Generation of Gravity Waves Associated with the Breaking of Mountain Waves. *Journal of the Atmospheric Sciences*, **56**, 3847–3858, https://doi.org/10.1175/1520-0469(1999)056<3847:SGOGWA>2.0.CO;2.

Schwartz, M. J., and Coauthors, 2008: Validation of the Aura Microwave Limb Sounder temperature and geopotential height measurements. *Journal of Geophysical Research*, **113**, D15S11, https://doi.org/10.1029/2007JD008783.

Semeniuk, K., and T. G. Shepherd, 2001a: Mechanisms for Tropical Upwelling in the Stratosphere. *Journal of the Atmospheric Sciences*, **58**, 3097–3115, https://doi.org/10.1175/1520-0469(2001)058<3097:MFTUIT>2.0.CO;2.

——, and ——, 2001b: The Middle-Atmosphere Hadley Circulation and Equatorial Inertial Adjustment. *Journal of the Atmospheric Sciences*, **58**, 3077–3096, https://doi.org/10.1175/1520-0469(2001)058<3077:TMAHCA>2.0.CO;2.

Shine, K. P., 1987: The Middle Atmosphere In the Absence of Dynamical Heat Fluxes. *Quarterly Journal of the Royal Meteorological Society*, **113**, 603–633, https://doi.org/10.1002/qj.49711347610.

Siskind, D. E., and J. P. McCormack, 2014: Summer mesospheric warmings and the quasi 2 day wave: Siskind and McCormack: Summer mesospheric warmings. *Geophysical Research Letters*, **41**, 717–722, https://doi.org/10.1002/2013GL058875.

Sjoberg, J. P., and T. Birner, 2014: Stratospheric Wave–Mean Flow Feedbacks and Sudden Stratospheric Warmings in a Simple Model Forced by Upward Wave Activity Flux. *Journal of the Atmospheric Sciences*, **71**, 4055–4071, https://doi.org/10.1175/JAS-D-14-0113.1.

Smith, A. K., 1992: Preconditioning for Stratospheric Sudden Warmings: Sensitivity Studies with a Numerical Model. *Journal of the Atmospheric Sciences*, **49**, 1003–1019, https://doi.org/10.1175/1520-0469(1992)049<1003:PFSSWS>2.0.CO;2.

——, 1996: Longitudinal Variations in Mesospheric Winds: Evidence for Gravity Wave Filtering by Planetary Waves. *Journal of the Atmospheric Sciences*, **53**, 1156–1173, https://doi.org/10.1175/1520-0469(1996)053<1156:LVIMWE>2.0.CO;2.

Strobel, D. F., 1978: Parameterization of the atmospheric heating rate from 15 to 120 km due to O_2 and O_3 absorption of solar radiation. *Journal of Geophysical Research*, **83**, 6225–6230, https://doi.org/10.1029/JC083iC12p06225.

Thayaparan, T., W. K. Hocking, J. MacDougall, A. H. Manson, and C. E. Meek, 1997: Simultaneous observations of the 2-day wave at London (43°N, 81°W) and Saskatoon (52°N, 107°W) near 91 km altitude during the two years of 1993 and 1994. *Annales Geophysicae*, **15**, 1324–1339, https://doi.org/10.1007/s00585-997-1324-3.

Tunbridge, V. M., D. J. Sandford, and N. J. Mitchell, 2011: Zonal wave numbers of the summertime 2 day planetary wave observed in the mesosphere by EOS Aura

Microwave Limb Sounder. *Journal of Geophysical Research*, **116**, D11103, https://doi.org/10.1029/2010JD014567.

Vadas, S. L., and H. Liu, 2009: Generation of large-scale gravity waves and neutral winds in the thermosphere from the dissipation of convectively generated gravity waves. *Journal of Geophysical Research: Space Physics*, **114**, A10310, https://doi.org/10.1029/2009JA014108.

——, and G. Crowley, 2010: Sources of the traveling ionospheric disturbances observed by the ionospheric TIDDBIT sounder near Wallops Island on 30 October 2007. *Journal of Geophysical Research: Space Physics*, **115**, A07324, https://doi.org/10.1029/2009JA015053.

——, D. C. Fritts, and M. J. Alexander, 2003: Mechanism for the Generation of Secondary Waves in Wave Breaking Regions. *Journal of the Atmospheric Sciences*, **60**, 194–214, https://doi.org/10.1175/1520-0469(2003)060<0194:MFTGOS>2.0.CO;2.

Venne, D. E., and J. L. Stanford, 1979: Observation of a 4–Day Temperature Wave in the Polar Winter Stratosphere. *Journal of the Atmospheric Sciences*, **36**, 2016–2019, https://doi.org/10.1175/1520-0469(1979)036<2016:OOATWI>2.0.CO;2.

Watanabe, S., Y. Tomikawa, K. Sato, Y. Kawatani, K. Miyazaki, and M. Takahashi, 2009: Simulation of the eastward 4-day wave in the Antarctic winter mesosphere using a gravity wave resolving general circulation model. *Journal of Geophysical Research*, **114**, D16111, https://doi.org/10.1029/2008JD011636.

Waters, J. W., and Coauthors, 2006: The Earth observing system microwave limb sounder (EOS MLS) on the aura Satellite. *IEEE Transactions on Geoscience and Remote Sensing*, **44**, 1075–1092, https://doi.org/10.1109/TGRS.2006.873771.

Wu, D. L., P. B. Hays, W. R. Skinner, A. R. Marshall, M. D. Burrage, R. S. Lieberman, and D. A. Ortland, 1993: Observations of the quasi 2-day wave from the High Resolution Doppler Imager on Uars. *Geophysical Research Letters*, **20**, 2853–2856, https://doi.org/10.1029/93GL03008.

——, E. F. Fishbein, W. G. Read, and J. W. Waters, 1996: Excitation and Evolution of the Quasi-2-Day Wave Observed in *UARS* /MLS Temperature Measurements.

Journal of the Atmospheric Sciences, **53**, 728–738, https://doi.org/10.1175/1520-0469(1996)053<0728:EAEOTQ>2.0.CO;2.

Wu, W.-S., R. J. Purser, and D. F. Parrish, 2002: Three-Dimensional Variational Analysis with Spatially Inhomogeneous Covariances. *Monthly Weather Review*, **130**, 2905–2916, https://doi.org/10.1175/1520-0493(2002)130<2905:TDVAWS>2.0.CO;2.

Yasuda, Y., K. Sato, and N. Sugimoto, 2015a: A Theoretical Study on the Spontaneous Radiation of Inertia–Gravity Waves Using the Renormalization Group Method. Part I: Derivation of the Renormalization Group Equations. *Journal of the Atmospheric Sciences*, **72**, 957–983, https://doi.org/10.1175/JAS-D-13-0370.1.

——, ——, and ——, 2015b: A Theoretical Study on the Spontaneous Radiation of Inertia–Gravity Waves Using the Renormalization Group Method. Part II: Verification of the Theoretical Equations by Numerical Simulation. *Journal of the Atmospheric Sciences*, **72**, 984–1009, https://doi.org/10.1175/JAS-D-13-0371.1.

——, F. Bouchet, and A. Venaille, 2017: A New Interpretation of Vortex-Split Sudden Stratospheric Warmings in Terms of Equilibrium Statistical Mechanics. *Journal of the Atmospheric Sciences*, **74**, 3915–3936, https://doi.org/10.1175/JAS-D-17-0045.1.

Yasui, R., K. Sato, and Y. Miyoshi, 2018: The Momentum Budget in the Stratosphere, Mesosphere, and Lower Thermosphere. Part II: The In Situ Generation of Gravity Waves. *Journal of the Atmospheric Sciences*, **75**, 3635–3651, https://doi.org/10.1175/JAS-D-17-0337.1.

Yiğit, E., P. Koucká Knížová, K. Georgieva, and W. Ward, 2016: A review of vertical coupling in the Atmosphere–Ionosphere system: Effects of waves, sudden stratospheric warmings, space weather, and of solar activity. *Journal of Atmospheric and Solar-Terrestrial Physics*, **141**, 1–12, https://doi.org/10.1016/j.jastp.2016.02.011.